

See discussions, stats, and author profiles for this publication at: <https://www.researchgate.net/publication/232227786>

# Predictive Models of Biohydrogen and Biomethane Production Based on the Compositional and Structural Features of Lignocellulosic Materials

ARTICLE in ENVIRONMENTAL SCIENCE & TECHNOLOGY · OCTOBER 2012

Impact Factor: 5.33 · DOI: 10.1021/es303132t · Source: PubMed

CITATIONS

47

READS

162

8 AUTHORS, INCLUDING:



**Cecilia Sambusiti**

French National Institute for Agricultural Rese...

33 PUBLICATIONS 241 CITATIONS

SEE PROFILE



**Abdellatif Barakat**

French National Institute for Agricultural Rese...

54 PUBLICATIONS 665 CITATIONS

SEE PROFILE



**Eric Trably**

French National Institute for Agricultural Rese...

74 PUBLICATIONS 1,217 CITATIONS

SEE PROFILE



**Hélène Carrere**

French National Institute for Agricultural Rese...

94 PUBLICATIONS 3,075 CITATIONS

SEE PROFILE

# Predictive Models of Biohydrogen and Biomethane Production Based on the Compositional and Structural Features of Lignocellulosic Materials

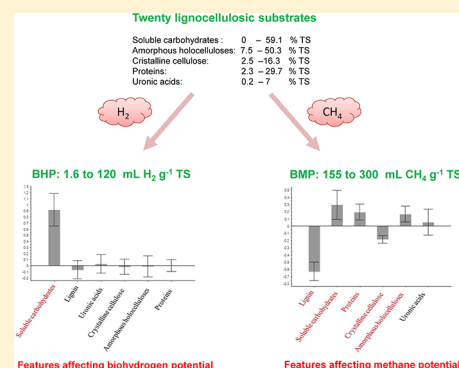
Florian Monlau,<sup>†</sup> Cecilia Sambusiti,<sup>‡</sup> Abdellatif Barakat,<sup>§</sup> Xin Mei Guo,<sup>†</sup> Eric Latrille,<sup>†</sup> Eric Trably,<sup>†</sup> Jean-Philippe Steyer,<sup>†</sup> and H  l  ne Carrere<sup>†,\*</sup>

<sup>†</sup>INRA, UR0050, Laboratoire de Biotechnologie de l'Environnement, Avenue des Etangs, 11100 Narbonne, France

<sup>‡</sup>DIAR, Environmental Section, Politecnico di Milano, Piazza L. da Vinci, 32, 20133, Milano, Italy

<sup>§</sup>INRA, UMR IATE 1208, Ing  nierie des Agro polym  res et Technologies Emergentes, 2, place Pierre Viala F- 34060 Montpellier, France

**ABSTRACT:** In an integrated biorefinery concept, biological hydrogen and methane production from lignocellulosic substrates appears to be one of the most promising alternatives to produce energy from renewable sources. However, lignocellulosic substrates present compositional and structural features that can limit their conversion into biohydrogen and methane. In this study, biohydrogen and methane potentials of 20 lignocellulosic residues were evaluated. Compositional (lignin, cellulose, hemicelluloses, total uronic acids, proteins, and soluble sugars) as well as structural features (crystallinity) were determined for each substrate. Two predictive partial least square (PLS) models were built to determine which compositional and structural parameters affected biohydrogen or methane production from lignocellulosic substrates, among proteins, total uronic acids, soluble sugars, crystalline cellulose, amorphous holocelluloses, and lignin. Only soluble sugars had a significant positive effect on biohydrogen production. Besides, methane potentials correlated negatively to the lignin contents and, to a lower extent, crystalline cellulose showed also a negative impact, whereas soluble sugars, proteins, and amorphous hemicelluloses showed a positive impact. These findings will help to develop further pretreatment strategies for enhancing both biohydrogen and methane production.



## INTRODUCTION

Development of new technologies for renewable energy generation such as biohydrogen and biomethane from lignocellulosic materials in a concept of integrated biorefinery appears to be very promising alternative to fossil fuels.<sup>1,2</sup> Worldwide, the lignocellulosic biomass was evaluated to be about 200 billion tons annually.<sup>3</sup> The use of lignocellulosic biomass and more particularly agricultural residues as bioenergy sources is interesting because of (i) its renewability, (ii) it provides additional incomes to farmers, (iii) it uses the nonedible part (stalks, leaves) of the plants and thus does not compete with food, and (iv) it permits us to treat residues that are often burned in the field creating environmental pollution.<sup>3,4</sup>

Methane is produced by a biological process in four steps (hydrolysis, acidogenesis, acetogenesis, and methanogenesis) – so-called anaerobic digestion. Biohydrogen is produced by dark fermentation that consists of an intermediate stage of anaerobic digestion where the last step of methanogenesis does not occur. Biohydrogen and methane can be produced using undefined mixed microbial cultures.<sup>2,5</sup> Mixed cultures are easier to use than pure cultures as they do not require aseptic conditions and can convert a large range of feedstocks into biohydrogen or methane.<sup>6,7</sup> Nevertheless, in the case of biohydrogen

production with mixed cultures, it is necessary to apply heat shock or chemical pretreatments to block the conversion of acetate or hydrogen and carbon dioxide into methane.<sup>5</sup>

Lignocellulosic substrates are composed of three main fractions: lignin, cellulose, and hemicelluloses. Contrary to lignin, the holocelluloses, that are cellulose and hemicelluloses, can be converted into biohydrogen and methane.<sup>2</sup> Nevertheless, lignocellulosic substrates present structural features that limit the accessibility of holocelluloses to microorganisms and thus their conversion to biohydrogen or methane.

Only a few studies have attempted to give some insights into the effect of compositional and structural features of lignocellulosic substrates on biohydrogen and methane production.<sup>8–12</sup> The correlations found in the literature between the composition of lignocellulosic residues and biohydrogen or methane production are summarized in Table 1.

For hydrogen production, Guo (2012) recently showed a good correlation ( $R^2 = 0.89$ ) between biohydrogen yields and

Received: August 1, 2012

Revised: October 3, 2012

Accepted: October 10, 2012

Published: October 10, 2012

**Table 1. Correlations Found in the Literature between the Compositional Characteristics of Lignocellulosic Substrates and Biohydrogen or Methane Production**

fermentation process	biomass used	compositional features	equation	refs
biohydrogen	organic solid substrates ( $n = 21$ )	soluble carbohydrates (Carb)	$BHP \text{ (mL } H_2 \cdot g^{-1} \text{ TS)} = 1.31 + 199.46 \text{ Carb}$	12
methane	manure ( $n = 10$ ), energy crops ( $n = 10$ )	lignin (Lig)	$BMP \text{ (L } CH_4 \cdot kg^{-1} \text{ VS)} = -1.67 * Lig + 421.7$	11
methane	raw and thermo-chemically pretreated sunflower stalks ( $n = 8$ )	lignin (Lig)	$BMP \text{ (L } CH_4 \cdot kg^{-1} \text{ VS)} = -0.65 * Lig + 379.8$	40
methane	lignocellulosic residues ( $n = 7$ )	soluble carbohydrates (Carb), acid detergent fiber (ADF), protein (Pro), lignin (Lig), ash (A)	$BMP \text{ (L } CH_4 \cdot kg^{-1} \text{ VS)} = 0.18 + 0.48 * CaRB + 0.2 * ADF - 0.003 * Lig / ADF + 2.8 \text{ Pro} - 0.83 * A$	8
methane	lignocellulosic residues ( $n = 12$ )	soluble carbohydrates (Carb), acid detergent fiber (ADF), protein (N), ash (A), lipids (F)	$BMP \text{ (L } CH_4 \cdot kg^{-1} \text{ VS)} = 0.045 + 1.23 * Carb + 0.24 * Pro + 1.51 * F - 0.68 * ADF - 0.81 * Cell - 6.1 * A$	9
methane	lignocellulosic residues ( $n = 15$ )	lignin (Lig)	biodegradability (%MV) = $0.83 - 1.82 * Lig$	39
methane	municipal solid waste ( $n = 2$ ), agricultural residues ( $n = 2$ ), manure ( $n = 4$ ), vegetables ( $n = 6$ )	lignin (Lig), cellulose (Cell)	biodegradability (%DCO) = $0.87 - 1.03 (\% \text{ lignin} + \% \text{ cellulose})$	10

soluble carbohydrates extracted under mild acid conditions (2 N hydrochloric acid).<sup>12</sup> The main bottleneck of using lignocellulosic biomass in dark fermentation processes is to convert holocelluloses into fermentable sugars.<sup>13</sup> Recently, Yuan et al. (2011) showed that hydrogen production from wheat straw was well correlated with the degradation of cellulose and hemicelluloses into fermentable sugars.<sup>14</sup> However, knowledge about the effect of compositional and structural features on biohydrogen potentials remains very limited.

According to Gunaseelan (2007), methane potentials can be predicted from five main chemical constituents (total soluble carbohydrate, acid detergent fibers (ADF), lignin/ADF, nitrogen, and ash), which accounted for 90% of the total variation in methane potentials ( $R^2 = 0.90$ ).<sup>8</sup> Negative correlations were also found between lignin contents and biochemical methane potentials for manure and energy crops ( $R^2 = 0.88$ ).<sup>11</sup> Similarly, Buffiere et al. (2006) showed a negative correlation between anaerobic biodegradability and the sum of cellulose and lignin contents.<sup>10</sup> In contrast, Eleazer et al. (1997) reported that methane potentials from several municipal solid wastes correlated positively to the sum of cellulose and hemicelluloses contents.<sup>15</sup> In all of these studies, lignin seemed to be the main restrictive factor for methane production, likely by limiting the microbial accessibility to holocelluloses during the fermentative process.<sup>2,16</sup> Overall, the effect of other compositional features, especially cellulose, is still not clear and sometimes contradictory between the different studies.

Except models established by Gunasselan (2007 and 2009), all models previously described were built with only one or two compositional characteristics.<sup>8,9</sup> Moreover, only compositional features have been considered and the effect of structural characteristics such as cellulose crystallinity has not been investigated yet. Indeed, cellulose presents both crystalline and amorphous parts and the crystalline one prevents plant cell penetration by micro-organisms or extracellular enzymes.<sup>17</sup> Other compositional characteristics such as the presence of pectin (polymer of uronic acids) have not been considered in models. Recently, Pakarinen et al. (2012) showed that pectin removal can significantly increase enzymatic hydrolysis of lignocellulosic substrates.<sup>18</sup>

Information about the influence of compositional and structural features on fermentative processes is thus limited especially for biohydrogen production, and sometimes results

are contradictory. So the determination of compositional (lignin, holocelluloses, uronic acids, and soluble fractions) and structural (crystallinity of cellulose) characteristics appears essential to understand the limitation of lignocellulosic material conversion into biohydrogen or methane. Moreover, this study can be valuable to obtain guidelines for establishing further pretreatment strategies to improve biohydrogen and methane production from lignocellulosic residues.

The objectives of this study were: (1) to characterize the compositional (cellulose, hemicelluloses, lignin, uronic acids, proteins, soluble carbohydrates) and structural features (crystallinity of cellulose) of various lignocellulosic substrates, (2) to evaluate their biohydrogen and methane potentials, and (3) to develop multilinear PLS models for predicting biohydrogen and methane potentials from their compositional and structural features.

## 2. MATERIALS AND METHODS

**2.1. Lignocellulosic Materials.** The substrates used in this study were selected among various lignocellulosic residues, biomass crops, and carbohydrate-rich substrates, but no lipid-rich substrate was considered. They corresponded to rice straw, giant reed (stalks and leaves), three varieties of sunflower stalks (1, 2, and 3), sunflower bark, sunflower oil cakes, maize (stalks, leaves, and cobs), Jerusalem artichoke (stalks, leaves, and tubers), and six varieties of sorghum (1, seed sorghum stalks; 2, biomass sorghum; 4, forage sorghum; 3, 5, and 6, sweet sorghum). All substrates were milled into particles of 2 mm using a cutting milling Restch, SM 100. The substrates were analyzed for total solids (TS) (Table 2) according to the APHA standard method.<sup>19</sup>

**2.2. Chemical Composition.** Soluble sugars (glucose and fructose) from starch, sucrose, and inulin were extracted using a mild acid hydrolysis method.<sup>20</sup> Samples (200 mg) were hydrolyzed at 121 °C, for 1h, with 0.2%  $H_2SO_4$ . The supernatant was filtrated with nylon filters (20  $\mu m$ ) and released carbohydrates (glucose and fructose) were quantified by high-pressure liquid chromatography (HPLC) method coupled to refractometric detection. The analysis was done with a combined Water/Dionex system (Ultimate 3000) using a Biorad HPX-87P column at 85 °C. The eluent corresponded to deionized water under a flow rate of 0.6 mL  $min^{-1}$ . The system was calibrated with glucose and fructose standards (Sigma–Aldrich).

Table 2. Compositional and Structural Features of Lignocellulosic Substrates and Validity Range of PLS Models, Values Correspond to the Means of Two Replicates of Independent Values  $\pm$  Standard Deviations (Error Bars)

substrates	Chemical Composition (% TS)						FTIR Spectra			
	% TS	SolSu	Pro	Ua	Hem	Cell	Lig	LOI	Cri (% TS)	Am (% TS)
rice straw	0.96	0.8	5.3 (±0.2)	0.6 (±0.1)	18.8 (±0.7)	26.2 (±0.5)	27 (±2.6)	0.85	12	33
giant reed stalks	0.99	0.3	4.3 (±0.7)	0.2 (±0.0)	18.5 (±0.7)	33.1 (±1.3)	24.5 (±0.1)	1.03	16.8	34.8
giant reed leaves	0.99	2.9	8 (±0.1)	0.7 (±0.1)	17.7 (±0.6)	20.9 (±0.6)	25.4 (±0.1)	0.95	10.2	28.4
sunflower stalks 1	0.94	0	4.8 (±0.1)	7.0 (±0.6)	15.6 (±0.3)	31 (±1.6)	29.2 (±1.6)	1.22	17	29.6
sunflower stalks 2	0.96	0	2.3 (±0.4)	3.9 (±0.4)	14.3 (±2.4)	31.2 (±3.1)	27.7 (±0.2)	1.2	17	28.4
sunflower stalks 3	0.96	0	4.3 (±0.7)	2.4 (±0.2)	14.3 (±0.7)	31.2 (±0.7)	30 (±1.7)	1.18	16.9	28.6
sunflower stalks bark	0.97	0	2.8 (±0.4)	1.7 (±0.3)	13.5 (±0.2)	27.4 (±0.4)	35 (±0.4)	1.1	14.4	26.5
sunflower oil cakes	0.94	5.2	29.7 (±3.4)	1.4 (±0.2)	8.2 (±0.2)	5.1 (±0.3)	22.3 (±2.8)	0.96	3.8	12.1
maize stalks	0.99	0.4	7.4 (±0.1)	0.7 (±0.1)	21.2 (±0.6)	27.1 (±0.9)	23.2 (±0.1)	1.14	14.5	33.9
maize leaves	0.99	0.3	6.7 (±0.6)	1.0 (±0.2)	28.6 (±3.3)	30.9 (±3.1)	20.4 (±0.6)	1.03	15.7	43.8
maize cobs	0.96	0.2	4.3 (±0.3)	0.7 (±0.1)	34.6 (±1.4)	29.8 (±1.2)	19.2 (±1.0)	0.89	14	50.3
Jerusalem artichoke stalks	0.96	32.9	2.8 (±0.3)	0.2 (±0.0)	8.8 (±3.1)	9.6 (±3.1)	20.3 (±0.0)	0.95	4.7	13.7
Jerusalem artichoke leaves	0.94	2.6	12.4 (±0.3)	0.7 (±0.1)	4.7 (±0.6)	8.8 (±1.4)	12.9 (±1.3)	1.22	4.8	8.6
Jerusalem artichoke tubers	0.98	59.1	10.4 (±0.2)	1.5 (±0.2)	5 (±0.0)	5.4 (±0.3)	12.3 (±0.1)	1.1	2.8	7.5
sorghum 1	0.95	0.4	4.6 (±0.1)	0.9 (±0.1)	26.1 (±0.1)	29.1 (±0.3)	22.5 (±1.6)	1.09	15.2	40
sorghum 2	0.91	15.4	6.5 (±0.0)	0.6 (±0.1)	19.4 (±1.3)	22.2 (±1.5)	21.4 (±0.3)	1.05	11.4	28.3
sorghum 3	0.91	18.5	8.1 (±0.0)	1.0 (±0.0)	20.9 (±1.6)	20.1 (±1.7)	18.5 (±0.9)	0.98	10.3	27.9
sorghum 4	0.94	8.2	8.2 (±0.0)	0.6 (±0.0)	21.7 (±0.2)	18.3 (±5.8)	20.7 (±3.0)	1.03	9.3	27.7
sorghum 5	0.92	22.8	6.9 (±0.0)	0.6 (±0.0)	20 (±1.2)	19.7 (±0.2)	19.8 (±1.3)	1.11	10.4	26.2
sorghum 6	0.88	21.3	6.2 (±0.0)	0.6 (±0.0)	18.5 (±0.8)	18.1 (±0.1)	21.3 (±0.0)	1.1	9.5	24.4
validity range		0–59.1	2.3–29.7	0.2–7	4.7–34.6	5.4–33.1	12.3–35		2.5–16.3	7.5–50.3

Structural-carbohydrates (glucose, xylose, arabinose, uronic acids) from cellulose, hemicelluloses, and pectins were measured using a strong acid hydrolysis method adapted from Effland et al. (1977).<sup>21</sup> Samples (200 mg) were first hydrolyzed with 12 M H<sub>2</sub>SO<sub>4</sub> acid for 2 h at room temperature and then diluted to reach a final acid concentration of 1.5 M and kept at 100 °C for 3 h. The insoluble residue was separated from the supernatant by filtration on fibreglass paper (GFF, WHATMAN). This insoluble residue was washed with 50 mL of deionized water and then placed in a crucible. The crucible and the fibreglass paper were dried at 100 °C during 24 h to determine by weighing the amount of Klason lignin. The supernatant was further filtrated with nylon filters (20 µm) and analyzed for quantification of monomeric carbohydrates. All monosaccharides (glucose, xylose, arabinose, uronic acids) were analyzed by HPLC coupled to refractometric detection. The analysis was carried out with a combined Water/Dionex system (Ultimate 3000), using a Biorad HPX-87H column at 50 °C. The eluent corresponded to 0.005 M H<sub>2</sub>SO<sub>4</sub> under a flow rate of 0.3 mL min<sup>-1</sup>. A refractive index detector (Waters 2414) was used to quantify the carbohydrates. The system was calibrated with glucose, xylose, arabinose, and uronic acids (galacturonic and glucuronic) standards (Sigma–Aldrich). Thereafter, cellulose and hemicelluloses contents were estimated as follows (eqs 1 and 2):

$$\text{cellulose (\%TS)} = \text{glucose (\%TS)} / 1.11 \quad (1)$$

$$\begin{aligned} \text{hemicelluloses (\%TS)} \\ = [\text{Xylose(\%TS)} + \text{arabinose (\%TS)}] / 1.13 \end{aligned} \quad (2)$$

where 1.11 is the conversion factor for glucose-based polymers (glucose) to monomers and 1.13 is the conversion factor for xylose-based polymers (arabinose and xylose) to monomers according to Petersson et al. (2007).<sup>22</sup> Proteins were determined by multiplying Total Kjeldhal Nitrogen (TKN) by 6.25. TKN was analyzed by the standard method using a Buchi digestion unit K438 and a Buchi 370-K distillator/titrator.

**2.3. Crystallinity Measurement Assessment.** Fourier transform infrared spectroscopy (FTIR) spectroscopy was used to determine the crystallinity of lignocellulosic materials. FTIR spectra were collected in the 4000–600 cm<sup>-1</sup> range using a Nexus 5700 spectrometer (ThermoElectron Corp.) with built-in diamond ATR single reflection crystal and with a cooled MCT detector. Spectra were recorded in absorption mode at 4 cm<sup>-1</sup> intervals with 64 scans at room temperature. Three spectra were recorded for each sample and all spectra were analyzed using *Omnic v7.3* software. Among the different FTIR bands, the bands at 1430 and 898 cm<sup>-1</sup> are sensitive to the amount of crystalline cellulose and amorphous cellulose, respectively.<sup>23</sup> The bands ratio H 1430/H 898 commonly called lateral order indice (LOI) can be used to determine the amount of crystalline cellulose. Using eqs 3 and 4, the crystalline cellulose content was estimated (eq 5).

$$\text{cellulose} = \text{crystalline cellulose} + \text{amorphous cellulose} \quad (3)$$

$$\text{LOI} = \text{crystalline cellulose} / \text{amorphous cellulose} \quad (4)$$

$$\text{crystalline cellulose (IR)} = \text{cellulose} \times \text{CrI}_{\text{IR}} \quad (5)$$

$$\text{Where } \text{CrI}_{\text{IR}} = \text{LOI} / (1 + \text{LOI})$$

To validate the use of FTIR spectra to assess cellulose crystallinity, crystallinity was also determined by a more common technology, as X-ray diffraction, on eight lignocellulosic substrates (giant reed stalks, sunflower stalks 1, maize stalks, rice straw, sorghum 1, Jerusalem artichoke stalks, maize cobs, and sunflower oil cakes). X-ray measurements were performed in a Philips Analytical X-diffractometer using Cu Ka radiation at  $k = 0.1540$  nm (40 kV, 40 mA). The measurements were carried out on powder compacted to small mats. DRX data were collected at  $2\theta$  angle range from 5° to 50° with a step interval of 0.02°. The degree of crystallinity was expressed as a percentage of crystallinity index (% CrI). The equation used to calculate the CrI was previously described by Segal et al. (1959) in the following form:<sup>24</sup>

$$\text{CrI}_{\text{DRX}} = (I_{002} - I_{\text{am}}) / I_{002} * 100 \quad (6)$$

where  $I_{002}$  corresponds to the counter reading at peak intensity at a  $2\theta$  angle of 22° and  $I_{\text{am}}$  the counter reading at peak intensity at  $2\theta$  angle of 16° in cellulose.  $I_{002} - I_{\text{am}}$  corresponds to the intensity of the crystalline peak and  $I_{002}$  is the total intensity after subtraction of the background signal measured without cellulose.<sup>25</sup> Crystalline cellulose was determined using the eq 7:

$$\text{crystalline cellulose (DRX)} = \text{cellulose} \times \text{CrI}_{\text{DRX}} \quad (7)$$

A good correlation ( $R^2 = 0.93$ ) was found between crystalline cellulose values determined by DRX and FTIR (Figure 1).

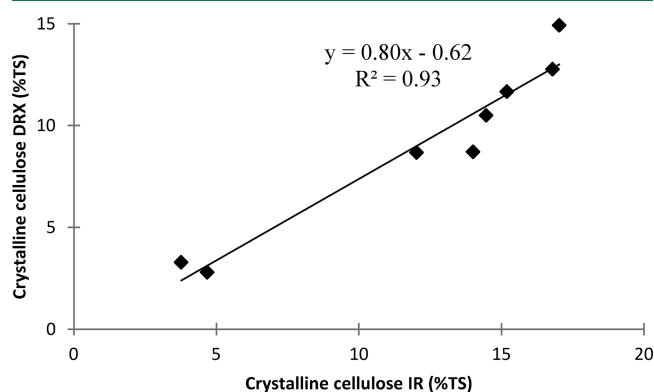


**Figure 1.** Correlation between crystalline celluloses determined by IR and DRX (expressed in %TS).

However, the amounts of crystalline cellulose determined by FTIR were higher than DRX, likely because  $\text{CrI}_{\text{IR}}$  measurements corresponded only to approximated values. Indeed, although 1430 and 898 cm<sup>-1</sup> bands are sensitive to the amount of crystalline cellulose and amorphous cellulose respectively, each band contains contributions from both crystalline and amorphous regions. Therefore, FTIR measurements must be considered as relative values and the FTIR method was only used to compare crystalline cellulose contents from different lignocellulosic materials.

**2.4. Biohydrogen and Methane Production.** **2.4.1. Bio-Hydrogen Potential (BHP).** BHP experiments were carried out in batch mode at 37 °C. The volume of each flask was 600 mL, with a working volume of 200 mL. A quantity of 3.5 g VS of substrate was initially introduced in each flask. Then, 200 mL of MES (2-[N-morpholino] ethane sulfonic acid, 50 mmol.L<sup>-1</sup>) buffer and 3 mL of seed sludge of an anaerobic digester (as inoculum) (final concentration around 225 mg-COD.L<sup>-1</sup>) were



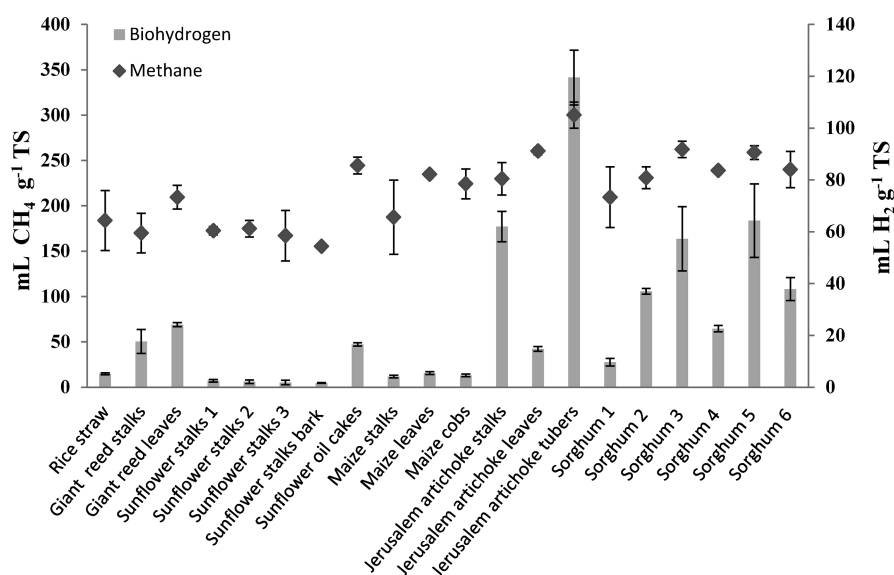


**Figure 2.** Biochemical biohydrogen and methane potentials of lignocellulosic substrates. Values correspond to the means of two replicates of independent values  $\pm$  standard deviations (error bars).

added to the flask. The inoculum was first treated at 90 °C for 15 min to inhibit the activity of methanogens and enrich in hydrogen producing bacteria. No additional nutrient medium solution was added. The initial pH value was adjusted to 5.5 with NaOH 2 N or 37% HCl. The headspace of the flasks was flushed with nitrogen gas to reach anaerobic conditions. The experimental procedure ended when the pressure in the flask headspace started to drop off indicating hydrogen consumption. Each experiment was performed in duplicates.

**2.4.2. Biochemical Methane Potential (BMP).** Lignocellulosic substrates were digested anaerobically in batch anaerobic flasks at 37 °C during 40 days. The volume of each flask was 600 mL, with a working volume of 400 mL. Each flask contained: 4.3 mL of a macroelement solution (NH<sub>4</sub>Cl, 26 g·L<sup>-1</sup>; KH<sub>2</sub>PO<sub>4</sub>, 10 g·L<sup>-1</sup>; MgCl<sub>2</sub>, 6 g·L<sup>-1</sup>; CaCl<sub>2</sub>, 3 g·L<sup>-1</sup>), 4 mL of a oligoelement solution (FeCl<sub>2</sub>, 2 g·L<sup>-1</sup>; CoCl<sub>2</sub>, 0.5 g·L<sup>-1</sup>; MnCl<sub>2</sub>, 0.1 g·L<sup>-1</sup>; NiCl<sub>2</sub>, 0.1 g·L<sup>-1</sup>; ZnCl<sub>2</sub>, 0.05 g·L<sup>-1</sup>; H<sub>3</sub>BO<sub>3</sub>, 0.05 g·L<sup>-1</sup>; Na<sub>2</sub>SeO<sub>3</sub>, 0.05 g·L<sup>-1</sup>; CuCl<sub>2</sub>, 0.04 g·L<sup>-1</sup>; Na<sub>2</sub>MoO<sub>4</sub>, 0.01 g·L<sup>-1</sup>), 20.8 mL of a bicarbonate buffer solution (NaHCO<sub>3</sub>, 50 g·L<sup>-1</sup>), an anaerobic sludge at 5 g VS·L<sup>-1</sup>, and the substrate at 5 g TS·L<sup>-1</sup>. Once the flasks were prepared, a degasification step with nitrogen gas was carried out to obtain anaerobic conditions. The bottles were closed with air impermeable red butyl rubber septum-type stoppers. Bottles were incubated at 35 °C and each experiment was carried out in duplicates.

**2.4.3. Gas Analysis.** Biogas volume was monitored continuously with a water displacement method. Acidified water (pH 2) was used to minimize dissolution of carbon dioxide. All volumes were expressed under temperature and pressure standard conditions. The gas composition (O<sub>2</sub>, CO<sub>2</sub>, CH<sub>4</sub>, H<sub>2</sub> and N<sub>2</sub>) was analyzed using a gas chromatograph (Clarus 580, PerkinElmer) equipped with two columns, a molecular sieve (Molsieve, 5 Å), and a thermal conductivity detector (TCD). One column (RtMolsieve) was used to separate H<sub>2</sub>, O<sub>2</sub>, N<sub>2</sub>, and CH<sub>4</sub>, and the second one (RtQBond) was used to separate CO<sub>2</sub> from other gases. The calibration was carried out with a standard gas (Linde) composed of 25% CO<sub>2</sub>, 2% O<sub>2</sub>, 10% N<sub>2</sub>, 5% H<sub>2</sub>, and 58% CH<sub>4</sub>.

**2.5. Partial Least-Squares Regression.** Partial least square (PLS) models were developed using *Unscrambler Version 10.2* software (CAMO software, A/S, Oslo, Norway). This method is particularly adapted for data with highly correlated variables. PLS models were used in full cross validation so-called leave-one-out cross validation procedure. This is a model validation method in which one sample is left out iteratively, a new calibration model is built, and then the sample that was left out is predicted using this model.<sup>26</sup> The iteration is continued until all samples are left once out of the calibration set. The prediction performances of the models were evaluated by calculating the coefficient of determination ( $R^2$ ) and the root-mean-square error of the calibration data set (RMSEPC). High  $R^2$  and low RMSEPC values indicate a good predictive robustness of the model. PLS models built were then tested on an independent set, and the root-mean-square error of independent validation set (RMSEPiv) was calculated to define the quality of the model. The RMSEP was defined as follow:

$$\text{RMSEP} = \sqrt{\frac{\sum_{i=1}^n (\hat{y}_i - y_i)^2}{n}} \quad (8)$$

where:  $\hat{y}_i$  is the prediction value of the sample  $i$  in a calibration data set (or independent validation set);  $y_i$  is the measured BHP or BMP value of the sample  $i$  in a calibration data set (or in a independent validation set) and  $n$  is the number of samples in calibration data set (or independent validation set).

### 3. RESULTS AND DISCUSSION

**3.1. Compositional and Structural Characteristics of the Lignocellulosic Substrates.** Soluble sugars (SolSu), uronic acids (Ua), proteins (Pro), hemicelluloses (Hem), cellulose (Cell), and lignin (Lig) contents of 20 lignocellulosic substrates are presented in Table 2, in % of TS. Soluble sugars (non structural carbohydrates like starch, sucrose and inulin) were mainly present in sorghum substrates (ranging from 8.2 to 22.8%, except for sorghum 1). Gunaseelan (2007) noticed as well a high content of soluble carbohydrates up to 23% of VS in

Table 3. External Validation of the PLS Models for Biohydrogen and Methane Potentials

independent samples	PLS Model for Biohydrogen Potentials				PLS Model for Methane Potentials			
	BHP measured mL H <sub>2</sub> g <sup>-1</sup> TS	BHP predicted mL H <sub>2</sub> g <sup>-1</sup> TS	errors	RMSEPiv	BMP measured mL CH <sub>4</sub> g <sup>-1</sup> TS	BMP predicted mL CH <sub>4</sub> g <sup>-1</sup> TS	errors	RMSEPiv
sorghum 1	9.7	9.2	4.5%	5.7	209.5	209	0.2%	6.7
sorghum 6	37.9	45.9	21.1%		240	230.5	4.0%	

sorghum bicolor roots.<sup>8</sup> According to Thuesombat et al. (2007), Jerusalem artichoke presents 70–90% of inulin (linear poly fructose chain), which explains the high values of soluble sugars found in Jerusalem artichoke stalks and tubers, that is, 32.9% and 59.1% per TS, respectively.<sup>27</sup> Proteins content ranged from 2.3% (sunflower stalk 2) to 29.7% (sunflower oil cakes). This result is consistent with Raposo et al. (2008), who evaluated a protein content of 31% per TS in sunflower oil cakes.<sup>28</sup> Uronic acids (galacturonic and glucuronic) that originated from both hemicelluloses and pectins were also quantified. Uronic acids contents ranged from 0.2% (giant reed and Jerusalem artichoke stalks) to 7% (sunflower stalks 1). Concerning the holocelluloses fraction, hemicelluloses content ranged from 5% (Jerusalem artichoke tubers) to 34.6% (maize cobs) and cellulose contents ranged from 5.4% (Jerusalem artichoke bulbs) to 33.1% (giant reed stalks). Crystalline cellulose and amorphous holocelluloses expressed in % TS using FTIR spectra are presented in Table 2. The crystalline cellulose content ranged from 2.5% for Jerusalem artichoke bulbs to 16.3% for giant reed stalks. The content of amorphous holocelluloses, which is the sum of amorphous cellulose and hemicelluloses, ranged from 7.5% (Jerusalem artichoke tubers) to 50.3% (maize cobs). Finally, lignin content ranged from 12.3% (Jerusalem artichoke tubers) to 35% (sunflower stalks bark). Moreover, on a same plant, lignin content was found higher in stalks than in leaves, except for giant reeds that presented almost similar lignin contents. Similar trends were observed with 14.1% and 18.4% of lignin for wheat straw leaves and stalks, respectively.<sup>29</sup> The range of the variables values (% per TS) is relatively high to permit to screen a wide range of compositional and structural features (Table 2).

**3.2. Biological Hydrogen Potential (BHP) and Biological Methane Potential (BMP) Tests.** Hydrogen and methane potentials of lignocellulosic substrates are presented in Figure 2. Biohydrogen potentials ranged from 1.6 (±0.1) mL H<sub>2</sub> g<sup>-1</sup>TS (sunflower stalk bark) to 120 (±11) mL H<sub>2</sub> g<sup>-1</sup>TS (Jerusalem artichoke tubers). Similarly to Jerusalem artichoke tubers, Jerusalem artichoke stalks presented an interesting biohydrogen potential as 62 (±6) mL H<sub>2</sub> g<sup>-1</sup> TS were produced. Except for sorghum 1, high sorghum hydrogen potentials from 23 (±1) mL H<sub>2</sub> g<sup>-1</sup> TS to 64 (±14) mL H<sub>2</sub> g<sup>-1</sup> TS were observed for sorghum substrates. Similar hydrogen yields were reported on sweet sorghum stalks with 52 mL H<sub>2</sub> g<sup>-1</sup> VS.<sup>30</sup> Sunflower stalks were found to produce low hydrogen potentials: 1.8 (±0.9), 2.1 (±0.7), and 2.5 (±0.5) mL H<sub>2</sub> g<sup>-1</sup> TS for sunflower stalks numbers 3, 2, and 1, respectively. With similar lignocellulosic residues, slightly lower hydrogen yields of 1 mL H<sub>2</sub> g<sup>-1</sup> VS and 3.16 mL H<sub>2</sub> g<sup>-1</sup> VS were observed for wheat straw and cornstalks, respectively.<sup>31,32</sup>

In addition, methane potentials ranged from 155 (±2) mL CH<sub>4</sub> g<sup>-1</sup> TS (sunflower stalks bark) to 300 (±14) mL CH<sub>4</sub> g<sup>-1</sup> TS (Jerusalem artichoke tubers). Such results are in agreement with literature data as Dinuccio et al. (2010) found methane potentials of 317 mL CH<sub>4</sub> g<sup>-1</sup> VS for maize residues, 229 mL CH<sub>4</sub> g<sup>-1</sup> VS for barley straw, and 195 mL CH<sub>4</sub> g<sup>-1</sup> VS for rice

straw.<sup>33</sup> Besides Jerusalem artichoke tubers, interesting methane production of 230 (±18) and 260 (±4) mL CH<sub>4</sub> g<sup>-1</sup> TS were observed for Jerusalem artichoke stalks and leaves, respectively. All sorghum substrates present methane potentials higher than 210 (±33) mL CH<sub>4</sub> g<sup>-1</sup> TS. Maize leaves and sunflower oil cakes also led to good methane potentials with respectively 235 (±3) and 244 (±9) mL CH<sub>4</sub> g<sup>-1</sup> TS. Low methane potentials were observed for the different varieties of sunflower stalks as 167 (±27), 172 (±5), and 175 (±9) mL CH<sub>4</sub> g<sup>-1</sup>TS for sunflower stalks numbers 3, 1, and 2, respectively. Moreover, on a same plant, the leaves appeared to have higher methane potentials than stalks. As an example, methane potentials of 170 (±22) and 210 (±13) mL CH<sub>4</sub> g<sup>-1</sup> TS were respectively observed for giant reed stalks and leaves, respectively. Overall, all results were lower than 480 mL CH<sub>4</sub>/kg TS, which is the theoretical methane potential of lignocellulosic substrates as proposed by Frigon and Guiof (2010).<sup>34</sup> Some biodegradable parts are indeed not accessible during anaerobic digestion of lignocellulosic substrates likely due to the compositional and structural characteristics that limit the accessibility of microorganisms to holocelluloses, as previously suggested by Triolo et al. (2011).<sup>11</sup>

**3.3. PLS Models.** One of the main objectives of this study was to identify the compositional and structural features affecting both biohydrogen and methane production from lignocellulosic residues, such as lignin (Lig), amorphous holocelluloses (Am), crystalline cellulose (Cri), protein (Pro), uronic acids (Ua), and soluble sugars (SolSu) contents. PLS models were built on eighteen lignocellulosic substrates and an independent validation set of two substrates (sorghum 1 and sorghum 6) was used to validate the PLS models. Table 2 shows the range values of the variables (Lig, Am, Cri, Pro, Ua, SolSu) in which PLS models are relevant and should not be extrapolated out of these ranges. In particular, the models should not be applied to lipid-rich substrates. Although these models are valid to estimate biohydrogen or methane yields in relation to compositional and structural features of lignocellulosic biomass, they provide no information about substrate degradation rates. Other abiotic and biotic factors such as pH, particle size, accessible surface area, porosity, moisture content, and so forth were not considered and may also impact biohydrogen and methane yields.

**3.3.1. Compositional and Structural Features Affecting Biohydrogen Production.** PLS analysis led to eq 9 as a multilinear model for biohydrogen potentials. The quality of the model to predict hydrogen potential was confirmed by a good R<sup>2</sup> (0.87) and a low value of RMSEPc (11.6 mL H<sub>2</sub> g<sup>-1</sup> TS).

$$\begin{aligned}
 \text{BHP}(\text{mL H}_2\text{g}^{-1}\text{TS}) &= 19.43 + 1.84 \cdot \text{SolSu}(\text{g. g}^{-1}\text{TS}) - 0.36 \cdot \text{Lig}(\text{g. g}^{-1}\text{TS}) \\
 &+ 0.53 \cdot \text{Ua}(\text{g. g}^{-1}\text{TS}) - 0.14 \cdot \text{Cri}(\text{g. g}^{-1}\text{TS}) \\
 &- 0.05 \cdot \text{Am}(\text{g. g}^{-1}\text{TS}) - 0.02 \cdot \text{Pro}(\text{g. g}^{-1}\text{TS}) \quad (9)
 \end{aligned}$$

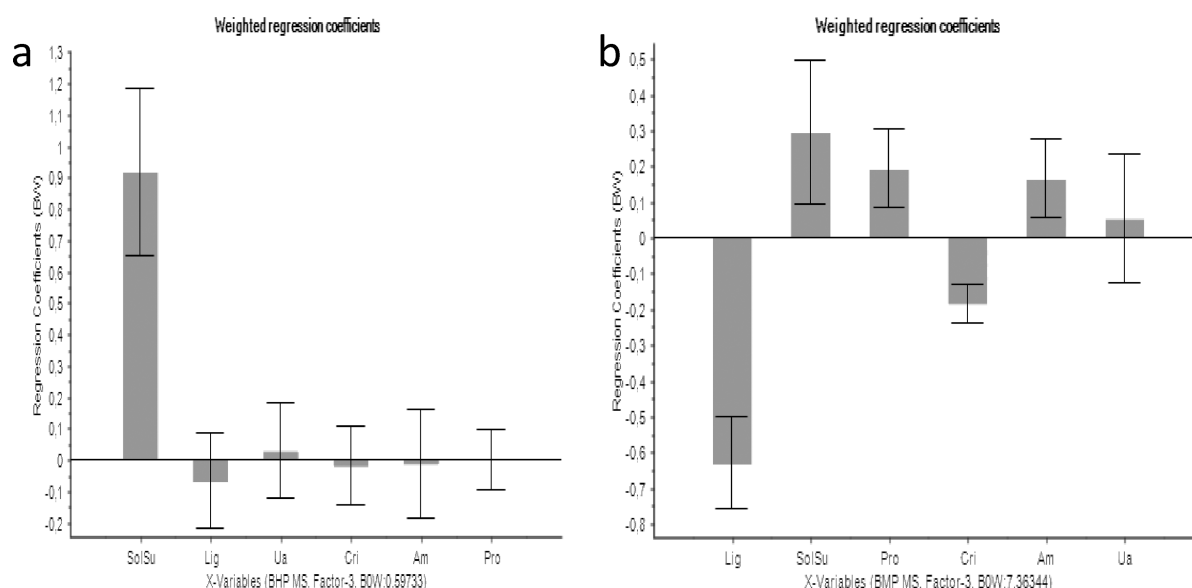


**Figure 3.** Centered and reduced regression coefficients with their 95% confidence intervals for the prediction of biohydrogen potentials (a), and methane potentials (b).

This model was validated using a set of two independent samples (sorghum 1 and sorghum 6, which were not included in the calibration data set. Results are presented in Table 3. Hydrogen potentials of 9.2 and 45.9 mL H<sub>2</sub> g<sup>-1</sup> TS were predicted compared to 9.7 and 37.9 mL H<sub>2</sub> g<sup>-1</sup> TS measured respectively for sorghum 1 and 6. The REMSEPIV was calculated on the validation data set and a promising result of 5.7 mL H<sub>2</sub> g<sup>-1</sup> TS was observed showing the high accuracy of the model.

Another interest of the PLS models is to determine which variables significantly impact the predicted variable. Centered and reduced weighted regression coefficients for hydrogen potentials are shown in part a of Figure 3. A strong positive correlation was found between hydrogen potentials and soluble sugars (SolSu) whereas all other studied variables (Lig, Am, Cri, Ua, Pro) had no significant impact. Considering the correlation of hydrogen production versus only soluble carbohydrates, a high correlation of  $R^2 = 0.95$  was observed (data not shown). These results are in accordance with Zhang et al. (2007), who suggested that hydrogen yield enhancement was due to an increase of soluble sugar content of the substrate.<sup>32</sup> Recently, Guo (2012) found a similar correlation ( $R^2 = 0.87$ ) between biohydrogen potentials and carbohydrates extracted under mild conditions (2 N hydrochloric acid).<sup>12</sup> Shi et al. (2012) suggested as well that the enhancement of hydrogen yields nearly coincided with an increase in water-soluble sugars available from alkali pretreated and raw sweet sorghum stalks, which were 2.23 and 0.86 g L<sup>-1</sup>, respectively.<sup>30</sup> Accordingly, Pan et al. (2011) showed that hydrolysis of cellulosic biomass led to an enhancement of hydrogen production due to an increase of soluble compounds that were much easier to be degraded.<sup>35</sup> In addition, our results showed that proteins did not affect hydrogen potentials within the range of studied protein contents (<30% TS, Table 2). This is consistent with Guo (2012), who reported that hydrogen potentials were lower in the case of protein-rich substrates but mainly because of their lower contents in carbohydrates.<sup>12</sup>

In addition, pH is an important factor that can affect biohydrogen production. Although the optimal pH for

hydrogen production from carbohydrates is rather acidic (about 4.5–6), alkaline pH (about 8.5–11) are more favorable for proteins-rich substrates.<sup>36,37</sup> In our study, the initial pH was set up at 5.5 that can explain the absence of significant effect of the proteins content. The absence of significant positive correlation between amorphous holocelluloses and hydrogen potentials can be explained by the poor efficiency of H<sub>2</sub>-producing bacteria to assimilate directly cellulosic materials. To achieve high yields of hydrogen from lignocellulosic substrates, a hydrolysis step is therefore required.<sup>38</sup>

**3.3.2. Compositional and Structural Features Affecting Methane Production.** PLS analysis led to eq 10 as a multilinear model for methane potentials. The quality of the model to predict methane potential was confirmed by a good  $R^2$  (0.88) and a low value of RMSEPC (14.9 mL CH<sub>4</sub> g<sup>-1</sup> TS).

$$\begin{aligned} \text{BMP}(\text{mL CH}_4 \text{ g}^{-1} \text{TS}) &= 303.14 - 4.53 * \text{Lig}(\text{g. g}^{-1} \text{TS}) \\ &+ 0.77 * \text{SolSu}(\text{g. g}^{-1} \text{TS}) + 1.28 * \text{Pro}(\text{g. g}^{-1} \text{TS}) \\ &- 1.59 * \text{Cri}(\text{g. g}^{-1} \text{TS}) + 0.61 * \text{Am}(\text{g. g}^{-1} \text{TS}) \\ &+ 1.33 * \text{Ua}(\text{g. g}^{-1} \text{TS}) \end{aligned} \quad (10)$$

This model was validated using an independent set of two samples (sorghum 1 and sorghum 6) which were not included in the calibration data set. Results are presented in Table 3. Errors of 0.2% and 4% between the experimental and predictive methane potentials were observed for sorghum 1 and sorghum 6, respectively. The REMSEPIV was calculated on the validation data set, and a result of 6.7 mL CH<sub>4</sub> g<sup>-1</sup> TS was observed showing the high accuracy of the models. Centered and reduced regression coefficients for the prediction of methane potentials are presented in part b of Figure 3. In this case, lignin, crystalline cellulose, soluble sugars, amorphous holocelluloses, and proteins contents were found to have a significant effect on methane potentials. A strong negative correlation was found between the lignin content and the methane production which is in agreement with other reported studies.<sup>11,39–41</sup> Kobayashi et al. (2004) showed a strong



negative correlation ( $R^2 = 0.95$ ) between the amount of methane produced and the amount of lignin of steam exploded bamboo.<sup>41</sup> Triolo et al. (2011) also found a high negative correlation ( $R^2 = 0.88$ ) between the lignin content and methane potentials of energy crops and manure.<sup>11</sup> However, our results led to a weak correlation ( $R^2$  of 0.82, data not shown) when considering only lignin content and methane potentials. Consequently, anaerobic biodegradation of lignocellulosic materials into methane is not only related to the lignin content, as suggested elsewhere.<sup>11</sup>

PLS regression showed that crystalline cellulose had also a negative impact on methane production but in a lower extent than lignin. Zhu et al. (2009) showed that lignin content and crystallinity are the two dominant parameters affecting negatively the digestibility of lignocellulosic substrates. Moreover, they suggested that cellulose crystallinity could have a higher influence on short time hydrolysis, whereas lignin content could have a higher impact on long time hydrolysis.<sup>42</sup>

Additionally, a significant positive correlation was found between methane potentials and the contents in soluble sugars, proteins and amorphous hemicelluloses in our study. According to Hayashi et al. (2005), the readily accessible regions (amorphous regions) of the lignocellulosic biomass are more efficiently hydrolyzed during enzymatic hydrolysis, resulting in the accumulation of crystalline cellulose.<sup>43</sup> Similarly, Scherer et al. (2000) showed that the most degradable part of spent grains corresponded to their soluble and hemicelluloses fractions, whereas cellulose and lignin were slightly degraded.<sup>44</sup> Besides, giving a quick tool to predict biohydrogen and methane potentials from lignocellulosic substrates, the PLS models built in this study are also valuable to give directions toward the development of pretreatments strategies of lignocellulosic residues for enhancing both biohydrogen and methane production. Pretreatments leading to the solubilization of holocelluloses might be recommended for enhancing biohydrogen production, whereas delignification, holocelluloses solubilization, and reducing crystalline cellulose may be recommended for methane production.

## AUTHOR INFORMATION

### Corresponding Author

\*Phone: +33 4 68 42 51 68, fax +33 4 68 42 51 60; e-mail: helene.carrere@supagro.inra.fr.

### Notes

The authors declare no competing financial interest.

## ACKNOWLEDGMENTS

The authors are grateful to ADEME, the French Environment and Energy Management Agency, for financial support in the form of F. Monlau's Ph.D. grant and to Dr. Solhy Abderrahim (INANOTECH Rabat) for his help in DRX analysis.

## REFERENCES

- (1) Kaparaju, P.; Serrano, M.; Thomsen, A. B.; Kongjan, P.; Angelidaki, I. Bioethanol, biohydrogen and biogas production from wheat straw in a biorefinery concept. *Bioresour. Technol.* **2009**, *100*, 2562–2568.
- (2) Monlau, F.; Barakat, A.; Trably, E.; Dumas, C.; Steyer, J.-P.; Carrere, H. Lignocellulosic materials into Biohydrogen and Bio-methane: impact of structural features and pretreatment. *Crit. Rev. Env. Sci. Tec.* **2012**, in press, DOI: 10.1080/10643389.2011.604258.

- (3) Ren, N.; Wang, A.; Cao, G.; Xu, J.; Gao, L. Bioconversion of lignocellulosic biomass to hydrogen: Potential and challenges. *Biotechnol. Adv.* **2009**, *27*, 1051–1060.
- (4) Sain, M.; Panthapulakkal, S. Bioprocess preparation of wheat straw fibers and their characterization. *Ind. Crop. Prod.* **2006**, *23*, 1–8.
- (5) Guo, X. M.; Trably, E.; Latrille, E.; Carrere, H.; Steyer, J. P. Hydrogen production from agricultural waste by dark fermentation: A review. *Int. J. Hydrogen Energ.* **2010**, *35*, 10660–10673.
- (6) Li, D. M.; Chen, H. Z. Biological hydrogen production from steam-exploded straw by simultaneous saccharification and fermentation. *Int. J. Hydrogen Energ.* **2007**, *32*, 1742–1748.
- (7) Ntaikou, I.; Antonopoulou, G.; Lyberatos, G. Biohydrogen production from biomass and wastes via dark fermentation: a review. *Waste and Biomass Valorization* **2010**, *1*, 21–39.
- (8) Gunaseelan, V. N. Regression models of ultimate methane yields of fruits and vegetable solid wastes, sorghum and napiergrass on chemical composition. *Bioresour. Technol.* **2007**, *98*, 1270–1277.
- (9) Gunaseelan, V. N. Predicting ultimate methane yields of *Jatropha curcus* and *Morus indica* from their chemical composition. *Bioresour. Technol.* **2009**, *100*, 3426–3429.
- (10) Buffiere, P.; Loisel, D.; Bernet, N.; Delgenes, J. P. Towards new indicators for the prediction of solid waste anaerobic digestion properties. *Water Sci. Technol.* **2006**, *53*, 233–241.
- (11) Triolo, J. M.; Sommer, S. G.; Moller, H. B.; Weisbjerg, M. R.; Jiang, X. Y. A new algorithm to characterize biodegradability of biomass during anaerobic digestion: Influence of lignin concentration on methane production potential. *Bioresour. Technol.* **2011**, *102*, 9395–9402.
- (12) Guo, X. M. *Biohydrogen production and metabolic pathways in dark fermentation related to the composition of organic solid waste*. Ph.D. Thesis, University of Montpellier, 2, 2012.
- (13) Cheng, C. L.; Lo, Y. C.; Lee, K. S.; Lee, D. J.; Lin, C. Y.; Chang, J. S. Biohydrogen production from lignocellulosic feedstock. *Bioresour. Technol.* **2011**, *102*, 8514–8523.
- (14) Yuan, X. Z.; Shi, X. S.; Zhang, P. D.; Wei, Y. L.; Guo, R. B.; Wang, L. S. Anaerobic biohydrogen production from wheat stalk by mixed microflora: Kinetic model and particle size influence. *Bioresour. Technol.* **2011**, *102*, 9007–9012.
- (15) Eleazer, W. E.; Odle, W. S.; Wang, Y. S.; Barlaz, M. A. Biodegradability of municipal solid waste components in laboratory-scale landfills. *Environ. Sci. Technol.* **1997**, *31*, 911–917.
- (16) Klimiuk, E.; Pokój, T.; Budzynski, W.; Dubis, B. Theoretical and observed biogas production from plant biomass of different fibre contents. *Bioresour. Technol.* **2010**, *101*, 9527–9535.
- (17) Fan, L.-T.; Lee, Y.-H.; Gharpuray, M. M. The nature of lignocellulosics and their pretreatments for enzymatic hydrolysis. *Adv. Biochem. Eng.* **1982**, *23*, 156–187.
- (18) Pakarinen, A.; Zhang, J.; Brock, T.; Majjala, P.; Viikari, L. Enzymatic accessibility of fiber hemp is enhanced by enzymatic or chemical removal of pectin. *Bioresour. Technol.* **2012**, *107*, 275–281.
- (19) (APHA), A. P. H. A. Standard Methods for the Examination of Water and Wastewater, 20th ed., 1998.
- (20) Nguyen, S.; Sophonputtanaphoca, S.; Kim, E.; Penner, M. Hydrolytic methods for the quantification of fructose equivalents in herbaceous biomass. *Appl. Biochem. Biotechnol.* **2009**, *158*, 352–361.
- (21) Effland, M. J. Modified procedure to determine acid-insoluble lignin in wood and pulp. *Tappi* **1977**, *60*, 143–144.
- (22) Petersson, A.; Thomsen, M. H.; Hauggaard-Nielsen, H.; Thomsen, A. B. Potential bioethanol and biogas production using lignocellulosic biomass from winter rye, oilseed rape and faba bean. *Biomass Bioenerg.* **2007**, *31*, 812–819.
- (23) Spiridon, I.; Teaca, C. A.; Bodirlau, R. Structural changes evidenced by ftir spectroscopy in cellulosic materials after pre-treatment with ionic liquid and enzymatic hydrolysis. *BioResources* **2010**, *6*, 400–413.
- (24) Segal, L.; Creely, J. J.; Martin, A. E., Jr; Conrad, C. M. An empirical method for estimating the degree of crystallinity of native cellulose using the X-ray diffractometer. *Textile Res. J.* **1959**, *29*, 786–794.

- (25) Park, S.; Baker, J. O.; Himmel, M. E.; Parilla, P. A.; Johnson, D. K. Cellulose crystallinity index: Measurement techniques and their impact on interpreting cellulase performance. *Biotechnol. Biofuels* **2010**, *3*, 10.
- (26) Raju, C. S.; Lokke, M. M.; Sutaryo, S.; Ward, A. J.; Moller, H. B. NIR monitoring of ammonia in anaerobic digesters using a diffuse reflectance probe. *Sensors* **2012**, *12*, 2340–2350.
- (27) Thuesombat, P.; Thanonkeo, P.; Laopaiboon, L.; Laopaiboon, P.; Yunchalard, S.; Kaewkannetra, P.; Thanonkeo, S. The batch ethanol fermentation of jerusalem artichoke using *saccharomyces cerevisiae*. *Sci. Tech. J.* **2007**, *7*.
- (28) Raposo, F.; Borja, R.; Rincon, B.; Jimenez, A. M. Assessment of process control parameters in the biochemical methane potential of sunflower oil cake. *Biomass Bioenerg.* **2008**, *32*, 1235–1244.
- (29) Fukushima, R. S.; Hatfield, R. D. Comparison of the acetyl bromide spectrophotometric method with other analytical lignin methods for determining lignin concentration in forage samples. *J. Agr. Food Chem.* **2004**, *52*, 3713–3720.
- (30) Shi, X. X.; Song, H. C.; Wang, C. R.; Tang, R. S.; Huang, Z. X.; Gao, T. R.; Xie, J. Enhanced bio-hydrogen production from sweet sorghum stalk with alkalization pretreatment by mixed anaerobic cultures. *Int. J. Energy Res.* **2010**, *34*, 662–672.
- (31) Fan, Y. T.; Zhang, Y. H.; Zhang, S. F.; Hou, H. W.; Ren, B. Z. Efficient conversion of wheat straw wastes into biohydrogen gas by cow dung compost. *Bioresour. Technol.* **2005**, *97*, 500–505.
- (32) Zhang, M. L.; Fan, Y. T.; Xing, Y.; Pan, C. M.; Zhang, G. S.; Lay, J. J. Enhanced biohydrogen production from cornstalk wastes with acidification pretreatment by mixed anaerobic cultures. *Biomass Bioenerg.* **2007**, *31*, 250–254.
- (33) Dinuccio, E.; Balsari, P.; Gioelli, F.; Menardo, S. Evaluation of the biogas productivity potential of some Italian agro-industrial biomasses. *Bioresour. Technol.* **2010**, *101*, 3780–3783.
- (34) Frigon, J. C.; Guiot, S. R. Biomethane production from starch and lignocellulosic crops: a comparative review. *Biofuels Bioprod. Bior.* **2010**, *4*, 447–458.
- (35) Pan, C. M.; Ma, H. C.; Fan, Y. T.; Hou, H. W. Bioaugmented cellulosic hydrogen production from cornstalk by integrating dilute acid-enzyme hydrolysis and dark fermentation. *Int. J. Hydrogen Energ.* **2011**, *36*, 4852–4862.
- (36) Cai, M. L.; Liu, J. X.; Wei, Y. S. Enhanced biohydrogen production from sewage sludge with alkaline pretreatment. *Environ. Sci. Technol.* **2004**, *38*, 3195–3202.
- (37) Xiao, B. Y.; Han, Y. P.; Liu, J. X. Evaluation of biohydrogen production from glucose and protein at neutral initial pH. *Int. J. Hydrogen Energ.* **2010**, *35*, 6152–6160.
- (38) Saratale, G. D.; Chen, S. D.; Lo, Y. C.; Saratale, R. G.; Chang, J. S. Outlook of biohydrogen production from lignocellulosic feedstock using dark fermentation - a review. *J. Sci. Ind. Res.* **2008**, *67*, 962–979.
- (39) Chandler, J. A.; Jewell, W. J.; Gossett, J. M.; Van Soest, P. J.; Robertson, J. B. Predicting methane fermentation biodegradability. *Biotechnol. Bioeng. Symp.* **1980**, 93–107.
- (40) Monlau, F.; Barakat, A.; Steyer, J. P.; Carrère, H. Comparison of seven types of thermo-chemical pretreatments on the structural features and anaerobic digestion of sunflower stalks. *Bioresour. Technol.* **2012**, *120*, 241–247.
- (41) Kobayashi, F.; Take, H.; Asada, C.; Nakamura, Y. Methane production from steam-exploded bamboo. *J. Biosci. Bioeng.* **2004**, *97*, 426–428.
- (42) Zhu, L.; O'Dwyer, J. P.; Chang, V. S.; Granda, C. B.; Holtzaple, M. T. Multiple linear regression model for predicting biomass digestibility from structural features. *Bioresour. Technol.* **2010**, *101*, 4971–4979.
- (43) Hayashi, N.; Kondo, T.; Ishihara, M. Enzymatically produced nano-ordered short elements containing cellulose I[beta] crystalline domains. *Carbohydr. Polym.* **2005**, *61*, 191–197.
- (44) Scherer, P. A.; Vollmer, G. R.; Fakhouri, T.; Martensen, S. Development of a methanogenic process to degrade exhaustively the organic fraction of municipal "grey waste" under thermophilic and hyperthermophilic conditions. *Water Sci. Technol.* **2000**, *41*, 83–91.